Ionomeric Blends of Poly(ethylene oxide) with Poly(styrene-*co*-maleic anhydride) Ionomer: Miscibility, Crystallization, and Melting Behavior

HASAN A. AL-SALAH

Polymer Science and Technology Research Lab, Chemistry Department, Mu'tah University, Mu'tah, Jordan

ABSTRACT: The miscibility and crystallization behavior of poly(ethylene oxide) (PEO) and poly(styrene-*co*-maleic anhydride) ionomer (SMAI) blends were studied by the dynamic mechanical analysis (DMA) and differential scanning calorimetry (DSC). This study has demonstrated that the presence of ion–dipole interactions enhances the miscibility of otherwise immiscible polymers in the PEO and high molecular weight poly(styrene-*co*-maleic anhydride) (SMA). The effect of ion–dipole interactions on enhancing miscibility is confirmed by the presence of a single glass transition temperature (T_g) and a depression of the equilibrium melting temperature of the PEO component. The equilibrium melting temperature of PEO in the blends are obtained using Hoffman-Weeks plots. The interaction energy density, β, is calculated from these data using the Nishi-Wang equation. The results suggest that PEO and SMAI blends are thermodynamically miscible in the melt. © 2000 John Wiley & Sons, Inc. J Appl Polym Sci 77: 1–7, 2000

Key words: PEO; SMAI; dynamic mechanical analysis; differential scanning calorimetry

INTRODUCTION

Multiphase polymer blends are of great importance in the development of new synthetic materials. However, the development of new useful alloys is severely limited by the strong immiscibility of many polymer pairs of interest. The miscibility of homopolymer/copolymer blends has been successfully achieved by the presence of specific intermolecular interactions.[1–4] These interactions include hydrogen bonding in bulk or solution,[5–10] and charge transfer complexes.[11–14]

Very recently, numerous studies have been focused on anion–cation and ion–dipole interactions as miscibility enhancers, and several systems have been subjected to these studies.[13–25] The systems that have been explored include the styrene–ethylacrylate system,[13] the styrene–isoprene system,[24] the polystyrene ionomer–poly(alkylene oxide) system,[16] nylon 4 and 6 with a polystyrene ionomer,[25–27] and poly(ethylacrylate-*co*-4-vinylpyridine) with a poly(ethylene terephthalate) anionomer.[17] In the literature a significant number of studies involving SMA are reported. SMA has been found to form miscible blends with some polymers.[29–32]

In our laboratory, it is of particular interest to study intermolecular complexes and crystallization as an extension to our studies on miscibility enhancements by introducing specific intermolecular interactions.[17,18,33] The miscible blends of semicrystalline PEO with oligomeric SMA has already been reported.[34] Because the entropy of mixing approaches zero for high molecular weight

polymer, SMA is no longer miscible with PEO. Blending will result in a two-phase material in which the high glass transition of the SMA remains unaffected. In this work, the results of a study will be presented in which ion–dipole interactions are used as miscibility enhancers. The purpose of this work is to examine the miscibility pattern of blends of poly(ethylene oxide) (PEO), a typical crystalline homopolymer, and high molecular weight of poly(styrene-*co*-maleic anhydride) ionomer (SMAI), the selected amorphous copolymer. A brief study will also be devoted to the exploration of the effect of ion content of SMAI and hydrogen bonding that are found in the carboxylic acid of hydrolyzed SMA on miscibility enhancement. The miscibility predictions are experimentally investigated by employing dynamic mechanical analysis (DMA), and differential scanning calorimetry (DSC). Furthermore, the crystallization behavior of the ionomer blends are analyzed in terms of Flory-Huggins theory.

EXPERIMENTAL

Materials

Poly(styrene-*co*-maleic anhydride) (SMA) containing 28 wt % maleic anhydride (MA) ($M_w = 110,000$, $M_n = 49,500$ g mol^{-1}), synthesized by free radical copolymerization was generously provided by DSM central research, Geleen, The Netherland. Poly(ethylene oxide) (PEO) was supplied by Aldrich; the viscosity-average molecular weight (M_v) was 100,000.

Synthesis of Poly(styrene-*co*-maleic anhydride) Ionomer (SMAI)

The maleic anhydride (MA) groups of SMA were partially hydrolyzed to carboxylate groups by dissolving SMA in a predetermined amount of NaOH aqueous ethanol solution. The mixture was refluxed for 24 h, cooled, and the ethanol removed. The polymer recovered by neutralizing the hydrolyzed polymer solution with HCl. The precipitated polymer was collected by filtration, dried at 60°C, and further dried under vacuum at 80°C. The carboxylic acid content was determined by titration using a standard solution of NaOH in methanol to a phenolphthalein end point following Erdi and Morawetz procedure.[35] The resulting hydrolyzed polymer was found to contain 10.6% malic acid, and designated as SMA-A10. Samples

of SMA-A10 in methanol were completely and partly neutralized by adding a precalculated amount of the methanolic NaOH to known concentration of SMA-A10 in methanol.

Blend Preparation and Methods of Analysis

The blends were prepared by dissolving calculated amounts of the two components in methanol to give about 20% (w/v) solutions. These solutions were stirred for about 12 h at ambient temperature. Films for physical testing were prepared by casting the polymer solutions in an aluminum mold that was coated with teflon. The films were air dried at 60°C for 48 h and then vacuum dried at 50°C for 48 h. All blend samples prepared are described in Table I.

Glass Transition Temperature Measurements

The glass transition temperatures (T_g) of samples were studied by using a TA 2000 instrument equipped with 910 differential scanning calorimetry (DSC) and 983 dynamic mechanical analysis (DMA). The DMA measurements were conducted on quenched samples prepared by compressing the dried films between two plates of a compression molding press under low pressure. The compression was carried out in the molten state for 2 min to remove the thermal history, followed by quenching to −120°C. Experiments were performed in the extension mode over the temperature range from −100°C until the sample became too soft, with a heating rate of 4°C/min and at a frequency of 10 Hz. The T_gs were taken as the relaxation peaks in the dissipation factor, tan δ, plots.

The glass transition temperature measurements by DSC were performed on 12 ± 2-mg samples under a dry nitrogen purge at a flow rate of 50 cm^3/min. The samples were first heated from ambient temperature to 200°C and maintained for 5 min before rapid quenching to liquid nitrogen temperature. The thermal behavior of the quenched samples were probed by heating from −100°C to the molten state at a heating rate of 10°C/min. The T_gs were taken as the midpoint of the change in heat capacity.

Melting Temperature and Crystallization

The melting temperature (T_m) were made on DSC calibrated with indium at a heating rate of 10°C/min under a dry nitrogen atmosphere. To determine the melting temperatures (T_m) of 12 ± 2-mg

Table I   Blend Compositions, Code, Glass Transition Temperature (T_g), and Observed Melting Temperature (T_m)

| Blend Composition | Code | (wt/wt) | T_g (K) | | | T_m (K) |
			DSC	DMA	Fox	
PEO/SMA	B-10	100/0	205	217	—	342.0
PEO/SMA	B-82	80/20	209	223(415)	—	343.0
PEO/SMA	B-64	60/40	215	229(411)	—	345.0
PEO/SMA	B-01	0/100	408	419	—	—
PEO/SMAI-Na(10)	BI-82	80/20	223	235	228	350.0
PEO/SMAI-Na(10)	BI-64	60/40	247	260	257	347.2
PEO/SMAI-Na(10)	BI-55	50/50	259	271	274	345.8
PEO/SMAI-Na(10)	BI-46	40/60	283	295	294	344.5
PEO/SMAI-Na(10)	BI-28	20/80	336	341	344	341.5
PEO/SMAI-Na(10)	BI-01	0/100	415	438	—	—
PEO/SMAI-Na(8)	BINa-8	50/50	257	265	—	345.0
PEO/SMAI-Na(6)	BINa-6	50/50	252	263	—	343.0
PEO/SMAI-Na(4)	BINa-4	50/50	248	259	—	341.0
PEO/SMAI-Na(2)	BINa-2	50/50	244	255	—	339.0
PEO/SMAI-Na(0)	BINa-0	50/50	241	251	—	337.0

samples crystallized isothermally at different temperatures (T_c), the samples were first melted at 100°C for 10 min to remove any previous traces of crystallinity. The samples were cooled to the desired T_c and maintained them temperature for 3 h and then reheated from 20 to 200°C. The melting temperatures were taken as the maximum of the endothermic transition.

RESULTS AND DISCUSSION

Glass Transition Temperature Behavior

It is well known that the glass transition temperature of polymer blends is the accepted method to establish blend miscibility. In blends between any two polymers in the amorphous state, the presence of a single T_g intermediate between those of the pure polymers confirms the miscibility of the system. Two experimental techniques, DMA and DSC, were employed to study the T_g behavior.

The miscibility behavior is examined by DMA, which offers a more sensitive probe to the smaller domain sizes of polymer blends.[36,37] Figure 1 shows the dissipation factor, tan δ, plotted against temperature for pure components and blends of SMA and PEO containing, respectively, 0, 40, 80, and 100% of the latter. The spectrum corresponding to the amorphous SMA shows a prominent relaxation with a high tan δ peak at the maximum, while PEO shows a small tan δ

peak at −56°C and another peak at 75°C corresponding to the melting transition. The spectra of polymer blend samples show two tan δ relaxation peaks and do not shift significantly with blend composition. This behavior indicates the absence of strong interactions between the polymer blend components. The tan δ spectra as a function of temperature of PEO/SMAI blends are plotted in Figure 2. In these systems, ion–dipole interactions play a major role, as can be seen in a single
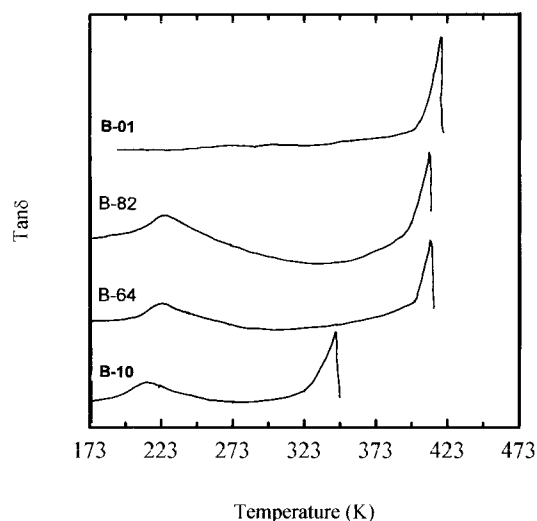

Figure 1 Temperature dependence of the dissipation factor, tan δ, for compression quenched-molded PEO/SMA blend samples.
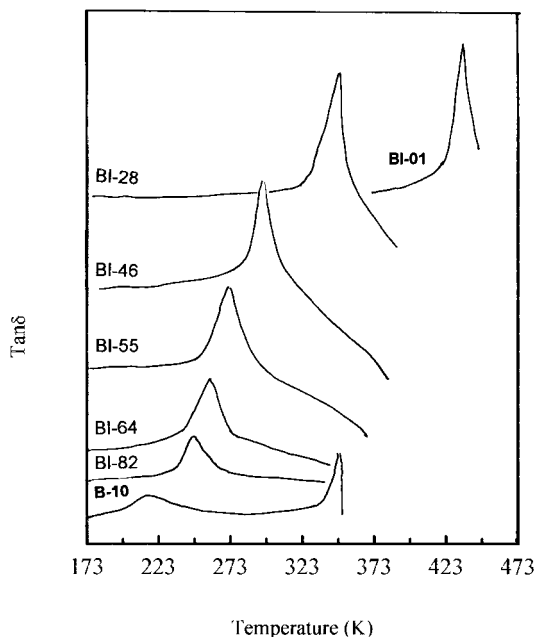
Figure 2 Temperature dependence of the dissipation factor, tan δ, for compression quenched-molded PEO/SMAI blend samples.

T_g and intermediate between the T_gs of the individual pure polymers. The temperature and the relaxation intensity of these peaks change with blend composition, giving higher temperatures and intensities as the amount of SMAI in the blend increases. These results clearly reflect a dramatic enhancement in miscibility in the presence of ionic groups.

The T_gs results for the PEO/SMAI ratio of 50/50 as a function of ion concentration are reported in Table I. All the binary blends show a single T_g and increase with increasing ion concentration. The results suggest that the presence of hydrogen bonding and ion–dipole interactions enhance the miscibility of otherwise immiscible polymers in the PEO/SMA blend system. In terms of the optical properties, the cloudiness of PEO and SMAI blend samples at room temperature is observed, and increases with increasing PEO content. Above melting temperature all the blend samples are completely clear.

Table I summarizes the T_g values of both pure and polymer blend samples obtained from DSC measurements. As can be seen, these results are consistent with the DMA test results, and the miscibility is enhanced by the strong ion–dipole interactions that limit the PEO chain mobility. In the literature, similar behavior has been reported for miscible PEO blend systems, where blends of

PEO/PMMA exhibit single T^gs that change with composition.[38–40] Li and Hsu[39] have reported that, when molten blends were quenched directly in the DSC, a single T_g was observed in all compositions, and these values fit the Fox equation[41] curve with some deviation for samples at high PEO content. In Figure 3, the T_g versus composition data on PEO/SMAI blends are replotted and compared with the simple predictions of Fox equation:

$$1/T_g = w_1/T_{g_1} + w_2/T_{g_2} \tag{1}$$

where w_i is the weight fraction of component i and Tg_i is its glass transition temperature. The subscripts 1 and 2 are used to designate the PEO and SMAI components, respectively.

Melting Temperature and Isothermal Crystallization

Typical DSC thermograms given in Figure 4 show the behavior of PEO/SMAI blends of various compositions after isothermal crystallization at 30°C for 3 h. The observed melting temperature (T_m) of PEO in PEO/SMAI as a function of blend composition is shown in Figure 5. The melting temperatures for all the blend samples crystallized at $T_c = 30$°C are summarized in Table I. The DSC data show that the melting temperature of PEO in PEO/SMAI blend samples decreases with the increase of the SMAI content. In general, the de-
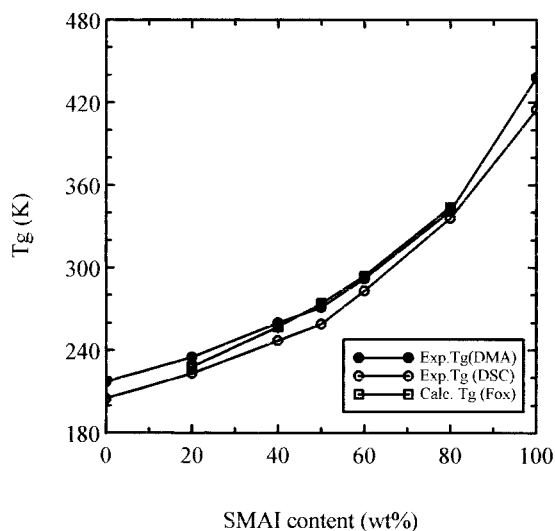

Figure 3 Glass transition temperature (T_g) versus composition of PEO/SMAI blend samples employing data from DSC, DMA, and the Fox equation.
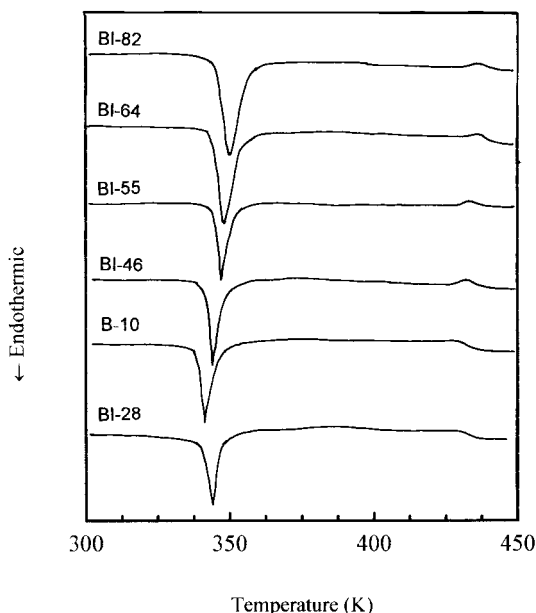
Figure 4 Typical DSC thermograms for PEO/SMAI blend samples recorded after isothermal crystallization at 30°C for 3 h.

crease in melting temperature of semicrystalline polymer (PEO) in blends can be due to morphological effects (decrease in lamellar thickness) and to thermodynamic factors (polymer–polymer interactions). From a thermodynamic factor point of view, the chemical potential of the crystalline
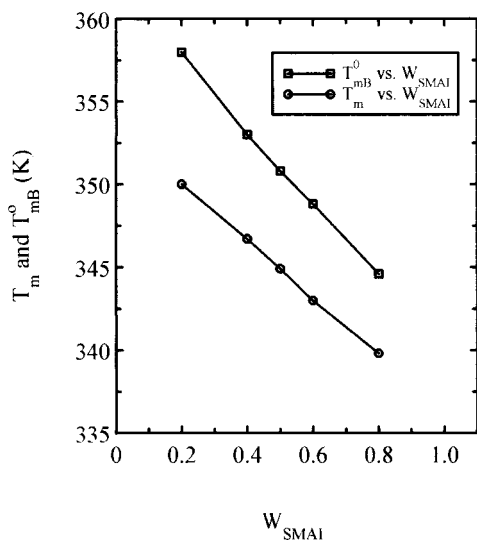

Figure 5 Plot of observed melting temperature (T_m) and equilibrium melting temperature (T_m°) of the PEO/SMAI blend samples crystallized at 30°C for 3 h versus weight fraction of SMAI.
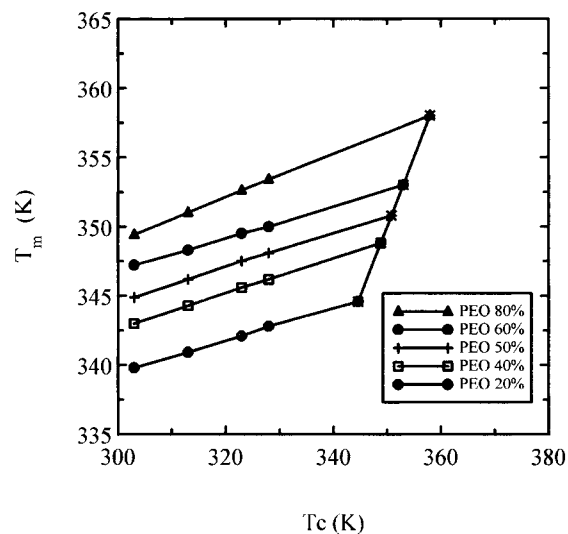

Figure 6 Plot of T_m versus T_c used to determine T_m°, for the different blend compositions.

polymer will be decreased by the addition of a amorphous miscible polymer. This fact will result in a decreased equilibrium melting temperature of the resulting blend. The equilibrium melting temperatures of crystallizable polymer blends can be obtained from the Hoffmann-Weeks equation.[42]

$$T_m = T_c/\eta + [1 - (1/\eta)]T_m^\circ \qquad (2)$$

where η is the ratio of the initial to the final lamellar thickness, T_m is the observed melting temperature, T_c is the isothermal crystallization temperature, and T_m° is the equilibrium melting temperature. Figure 6 shows the plots of the T_m versus T_c for the different PEO/SMA–ionomer blends. As observed, a good linear correlation between T_m and T_c is obtained. According to the Hoffman and Weeks analysis, the equilibrium melting temperature, T_m°, could be determined by extrapolation of T_m versus T_c to $T_m = T_c$ A fit of the data shown in Figure 6 yields the values for T_m° that are summarized in Table II. The slope of these straight lines gives almost constant value of $1/\eta$, and is independent of blend composition. For pure PEO, a value of $T_m^\circ = 345$ K is obtained. The high melting temperature found for pure PEO, 345 K, is indicative of very high molecular weight PEO, and agrees well with literature data.[34,43,44]

The melting point depression observed for the PEO can be used to estimate the polymer–polymer interaction parameter, χ_{12}, following the

Table II   Observed Melting Temperature (T_m) and Equilibrium Melting Temperature (T_m^0) as a Function of PEO/SMAI Blend Composition φ_1^2

Blend Composition	Code		Melting Temperature (K)		
		(wt/wt)	T_m	T_m^0	φ_1^2
PEO/SMAI-Na(10)	BI-10	100/0	342.0	345.0	—
PEO/SMAI-Na(10)	BI-82	80/20	350.0	358.0	0.03
PEO/SMAI-Na(10)	BI-64	60/40	347.2	353.0	0.13
PEO/SMAI-Na(10)	BI-55	50/50	345.8	350.8	0.21
PEO/SMAI-Na(10)	BI-46	40/60	344.5	350.0	0.31
PEO/SMAI-Na(10)	BI-28	20/80	341.5	344.6	0.60
PEO/SMAI-Na(10)	BI-01	0/100	—	—	—

thermodynamic treatment elaborated by Scott,[45] Nishi and Wang[46] and later by Imken et al.[47] The melting point depression of the crystalline polymer blended with an amorphous polymer in a miscible blend can be written as

$$(1/T_{mB}^\circ - 1/T_m^\circ) = -R/\Delta H_f(v_{2\mu}/v_{1\mu})$$
$$\times\,[\ln\ddot{o}_2/x_2 + (1/x_2 - 1/x_1)$$
$$(1 - \ddot{o}_2) + \chi_{12}\ddot{o}_1^2] \quad (3)$$

where T_{mB}° and T_m° are the equilibrium melting temperatures in the blend and of pure PEO, respectively, $v_{1\mu}$ and $v_{2\mu}$ are the molar volumes of the repeating unit of the amorphous and crystallizable components, H_f is the heat of fusion per mol of 100% crystalline PEO, x_1, $\ddot{o}_1$ and x_2, $\ddot{o}_2$ are the degree of polymerization and volume fractions of amorphous polymer 1 and crystallizable polymer 2, respectively. When x_1 and x_2 are both large and there are no entropic contributions to the melting point depression, then eq. (3) reduces to

$$(1/T_{mB}^\circ - 1/T_m^\circ) = -R/T\Delta H_f(v_{2\mu}/v_{1\mu})(\beta\ddot{o}_1^2) \quad (4)$$

where β is the interaction energy density and is related to the χ_{12} by

$$\beta = RT\chi_{12}/v_{1\mu} \quad (5)$$

upon rearranging with $T = T_{mB}^\circ$

$$(1 - T_{mB}^\circ/T_m^\circ) = -\beta v_{2\mu}/\Delta H_f(\ddot{o}_1^2) \quad (6)$$

If χ_{12} is composition independent and the melting point depression is not influenced by morphological effects, then a plot of the left-hand side of eq. (6) versus $\ddot{o}_1^2$ should give a straight line pass-

ing through the origin. Figure 7 shows such a plot and from the least squares line the intercept at origin of -0.0337 and slope of 0.063. This line does not pass through the origin, and can be accounted for by a composition dependence of χ_{12}.

By using eq. (6), the parameter $\Delta H_f/v_{2\mu}$ = 23.13 cal/cm^3,[48] and the slope of the line of Figure 7, the β value is -1.46 cal/cm^3. The interaction parameter could not be calculated because the datum of $v_{1\mu}$ is unavailable. But from eq. (6) and the β value found, it can be shown that $\chi_{12} < 0$. The negative value of χ_{12} strongly suggests that in the melt, at T_m, PEO, and SMAI are miscible.
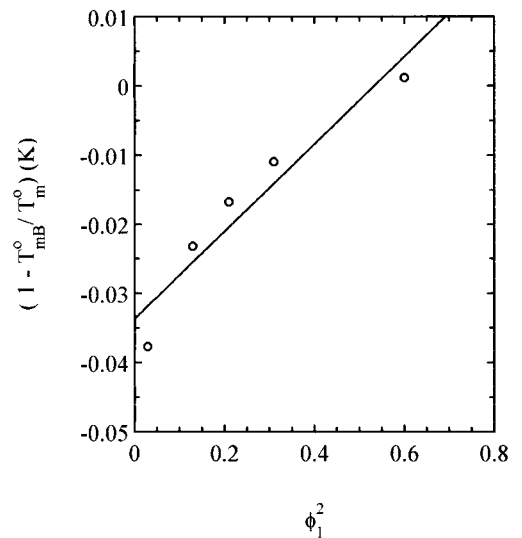
Figure 7   Plot of $(1 - T_{mB}^\circ/T_m^\circ)$ versus φ_1^2 for the PEO/SMAI blend system.

REFERENCES

1. Paul, D. R.; Newman, S. Polymer Blends; Academic Press: New York, 1978.
2. Cooper, S. L.; Estes, G. M., Eds. Multiphase Polymers; Adv. Chem. Ser. 176; American Chemical Society: Washington, DC, 1979.
3. Utracki, L. A. Polymer Alloys and Blends: Thermodynamics and Rheology; Hanser: Munich, 1990.
4. Dubin, P.; et al., Eds. Macromolecular Complexes in Chemistry and Biology; Springer Verlag: Berlin, 1994.
5. Djadoun, S.; Goldberg, R. N.; Morawetz, H. Macromolecules 1977, 10, 1015.
6. Xing, P.; Dong, L.; An, Y.; Feng, Z.; Avella, M.; Martuscelli, E. Macromolecules 1997, 30, 2726.
7. Lezcano, E. G.; Salom Coll, C.; Prolongo, M. G. Polymer 1996, 37, 3603.
8. Nishio, V.; Haratani, T.; Takahashi, T. J Polym Sci Polym Phys 1990, 28, 355.
9. Painter, P. C.; Veytsman, B.; Kumar, S.; Shenoy, S.; Graf, J. F.; Xu, Y.; Coleman, M.M. Macromolecules 1997, 30, 932.
10. Xiang, M.; Jiang, M.; Zhang, Y.; Wu, C.; Feng, L. Macromolecules 1997, 30, 2313.
11. Sulzberg, T.; Cotter, R. J. J Polym Sci Polym Chem 1970, 8, 2747.
12. Ohno, N.; Kumanotani, J. Polym J 1979, 11, 947.
13. Smith, P.; Eisenberg, A. J Polym Sci Polym Lett Ed 1983, 21, 223.
14. Rutkowska, M.; Eisenberg, A. Macromolecules 1984, 17, 821.
15. Horrion, J.; Jérôme, R.; Teyssié, J. Ph. J Polym Sci Polym Lett Ed 1986, 24, 69.
16. Hara, M.; Eisenberg, Ai. Macromolecules 1984, 17, 1335.
17. Al-Salah, H. A.; Xiao, H. X.; McLean, J. A.; Frisch, K. C. Polym Int 1992, 28, 323.
18. Al-Salah, H. A.; Al-Raheil, I. A. J Appl Polym Sci 1992, 45, 1661.
19. Kim, J. S.; Roberts, S. B.; Eisenberg, A.; Moore, R. B. Macromolecules 1993, 26, 5256.
20. Plante, M.; Bazuin, C. G.; Jérôme, R. Macromolecules 1997, 28, 1567.
21. Plante, M.; Bazuin, C. G. Macromolecules 1997, 30, 2613.
22. Choi, K.; Jo, W. H. Macromolecules 1997, 30, 1509.
23. Al-Salah, H. A. Polym Bull, accepted for publication.
24. Zhou, Z. L.; Eisenberg, A. J Polym Sci Polym Phys 1983, 21, 5951.
25. Ng, C. W. A.; Bellinger, M. A.; MacKnight, W. J. Macromolecules 1994, 27, 6942.
26. Molnar, A.; Eisenberg, A. Macromolecules 1992, 25, 5774.
27. Lu, X.; Weiss, R. A. Macromolecules 1992, 25, 6185.
28. Ng, C.; MacKnight, W. J. Macromolecules 1996, 29, 2412.
29. Dafieuw, G.; Groeninckx, G.; Reynaers, H. Polym Commun 1989, 30, 267.
30. Brannock, G. R.; Barlow, J. W.; Paul, D. R. J Polym Sci Polym Phys Ed 1991, 29, 413.
31. Koning, C.; Ikker, A.; Borggreve, R.; Lecmans, L.; Möller, M. Polymer 1993, 34, 4410.
32. Feng, H.; Shen, L.; Feng, Z. Eur Polym J 1995, 31, 243.
33. Al-Salah, H. A., in preparation.
34. Al-Salah, H. A.; Qudah, A. M. A. Polym Int 1997, 42, 429.
35. Erdi, N. Z.; Morawetz, H. J Colloid Sci 1964, 19, 708.
36. de Juana, R.; Hernandez, R.; Peña, J. J.; Santamaria, A.; Cortazar, M. Macromolecules 1994, 27, 6980.
37. Murayama, T. Dynamical Mechanical Analysis of Polymeric Materials; Elsevier: New York, 1978.
38. Liberman, S. A.; Gomes, A. D.; Macchi, E. M. J Polym Sci Polym Chem Ed 1984, 22, 2809.
39. Li, X.; Hsu, S. L. J Polym Sci Polym Phys Ed 1984, 22, 1331.
40. Silvestre, C.; Cimmino, S.; Martuscelli, E.; Karasz, F. E.; MacKnight, W. J. Polymer 1987, 28, 1190.
41. Fox, T. G. Bull Am Phys Soc 1956, 2, 123.
42. Hoffman, J. D.; Week, J. J. J Res Natt Bur Stand USA 1962, 66, 13.
43. Nedkov, E.; Kresteva, M.; Mihailov, M.; Todorova, U. J Macromol Sci Phys 1082, B21, 327.
44. Alfonso, G. C.; Russell, P. Macromolecules 1986, 19, 1143.
45. Scott, R. L. Chem Phys 1949, 17, 279.
46. Nishi, T.; Wang, T. T. Macromolecules 1975, 8, 909.
47. Imken, R. L.; Paul, D. R.; Barlow, J. W. Polym Eng Sci 1976, 16, 593.
48. Martuscelli, E.; Pracella, M.; Yue, W. P. Polymer 1984, 25, 1097.